SUPPLEMENTARY INFORMATION
Photoemission study of twisted monolayers and bilayers of WSe_2 on graphite substrates

Bharti Parashar,[1] Lars Rathmann,[2] Hyun-Jung Kim,[3] Iulia Cojocariu,[1] Aaron Bostwick,[4] Chris Jozwiak,[4] Eli Rotenberg,[4] José Avila,[5] Pavel Dudin,[5] Vitaliy Feyer,[1] Bernd Beschoten,[2,6] Christoph Stampfer,[2] Gustav Bihlmayer,[3] Claus M. Schneider,[1,7,8] and Lukasz Plucinski[1,*]

[1] *Peter Grünberg Institut (PGI-6), Forschungszentrum Jülich GmbH, 52428 Jülich, Germany*
[2] *2nd Institute of Physics and JARA-FIT and, RWTH Aachen University, 52074 Aachen, Germany*
[3] *Peter Grünberg Institut (PGI-1), Forschungszentrum Jülich GmbH, 52428 Jülich, Germany*
[4] *Advanced Light Source, Lawrence Berkeley National Laboratory, One Cyclotron Road, Berkeley, CA 94720, USA*
[5] *Synchrotron-SOLEIL, Université Paris-Saclay, Saint-Aubin, BP48, F91192 Gif sur Yvette, France*
[6] *JARA-FIT Institute for Quantum Information, Forschungszentrum Jülich GmbH and RWTH Aachen University, 52074 Aachen, Germany*
[7] *Fakultät für Physik, Universität Duisburg-Essen, 47048 Duisburg, Germany*
[8] *Physics Department, University of California, Davis, CA 95616, USA*

(Dated: December 18, 2022)

* l.plucinski@fz-juelich.de

SI. IDENTIFICATION OF SL AND BL MICRO-REGIONS ON SAMPLE B

The optical micrograph of sample B is presented in Fig. S1(a). We acquired a spatial map of ARPES intensity using capillary micro-focusing at $h\nu = 147$ eV at the MAESTRO beamline, as shown in Fig. S1(b). The numbered white boxes in Fig. S1(b) indicate the direction of the line-scan spectra and the positions at which we collected the data set.

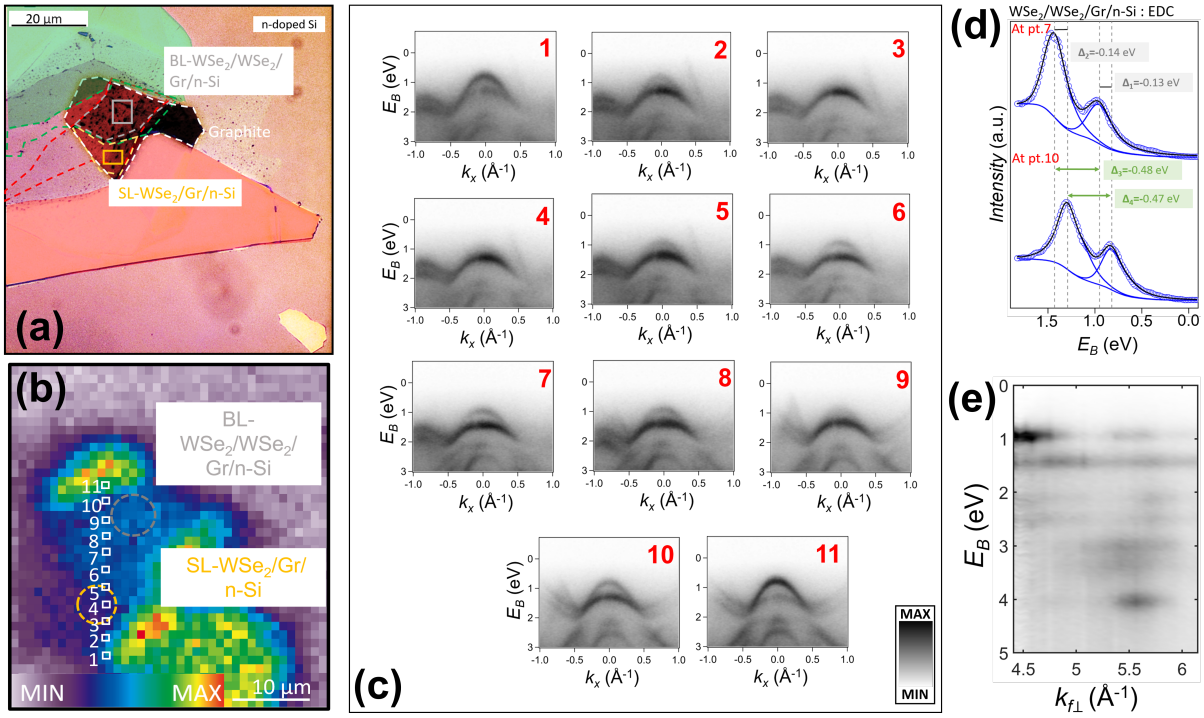

Figure S1. Characterization of sample B. (a) Optical micrograph of the twisted SL and BL WSe_2/graphite/n-Si. (b) Spatial photoemission intensity map of an integrated intensity of the valence band at the momenta related to WSe_2. (c) Collection of normal emission ARPES spectra at white boxes indicated in (b). (d) EDC profiles at boxes 7 and 10. (e) Set of normal emission spectra from twisted BL WSe_2/graphite for $h\nu$ between 80 and 150 eV with 2 eV step, with perpendicular momentum calculated as $k_{f\perp} = \sqrt{(E_{kin} + V_0)2m/\hbar^2}$, and V_0 set to 10 eV.

Figure S1(c) depicts a set of ARPES maps at 11 boxes indicated in panel Figure S1(b). $E(k)$ maps measured at normal emission at boxes 1, 6, 7, 8, 10, 11 show double bands and at boxes 3, 4 show single band near the VBM, which are characteristics signatures of the bilayer and monolayer regions, respectively. This indicates that also in sample B we were able to exclusively probe either SL or BL areas by changing the location of the beam position on the sample surface. For the BL regions, we measured binding energy shifts of the order of ~ 130 meV between points 7 and 10. The peak positions are confirmed by the Voigt fit of normal emission EDCs, Fig. S1(d). This indicates inhomogeneities and local doping on the flake surface that vary on the μm scale. Figure S1(e) presents the photon energy dependence $E_B(k_\perp)$ map on sample B showing virtually the same features as sample A (Fig. 1(f)), even though both samples have different twist angles between the WSe_2 monolayers.

SII. NANOARPES MEASUREMENTS AT ANTARES

Sample A had been characterized at the ANTARES beamline at SOLEIL synchrotron. As seen in Fig. S2(a), utilizing nanoAPRES in the imaging mode, different regions of the WSe_2 flake can be distinguished. The electronic band structure could be acquired using the nanoARPES beamline in spectroscopic mode, as shown in Fig. S2(b,c), which depict the band dispersion of monolayer and bilayer regions. At the high symmetry Γ_0 point, the monolayer region exhibits a single band at the local valence band maximum. In the bilayer region, the band is split into two branches. The observed results at ANTARES beamline are in agreement with those presented in the main paper, obtained at the MAESTRO beamline.

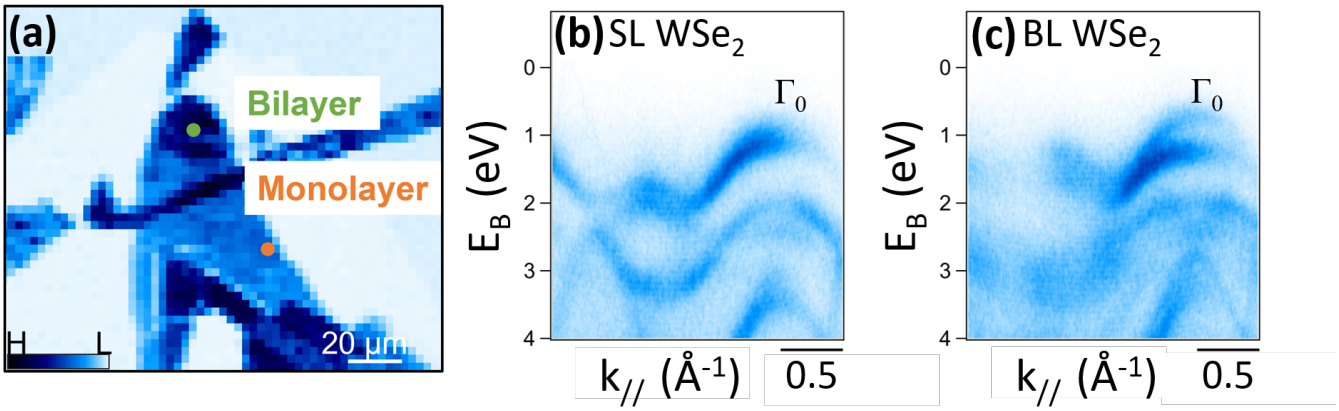

Figure S2. Band structure of different regions of WSe_2 flake by nanoARPES at ANTARES/SOLEIL. Panel (a) shows the nanoARPES image obtained by integrating intensity from 0.5 eV to 0.9 eV. Panels (b,c) show the band dispersion taken at $h\nu = 100$ eV along the Γ-K direction of the Brillouin zone from the two regions labeled in panel (a) by green and orange dots.

SIII. SAMPLE C: TWISTED SL WSE_2/GRAPHITE

Sample C was fabricated by mechanical exfoliation and dry transfer techniques. The WSe_2 monolayer was exfoliated from bulk crystal and transferred such that it partially covered two different substrates, graphite and n-Si. The overlapping area between WSe_2 layers and graphite is larger than 20×20 μm^2 as shown in Fig. S3.

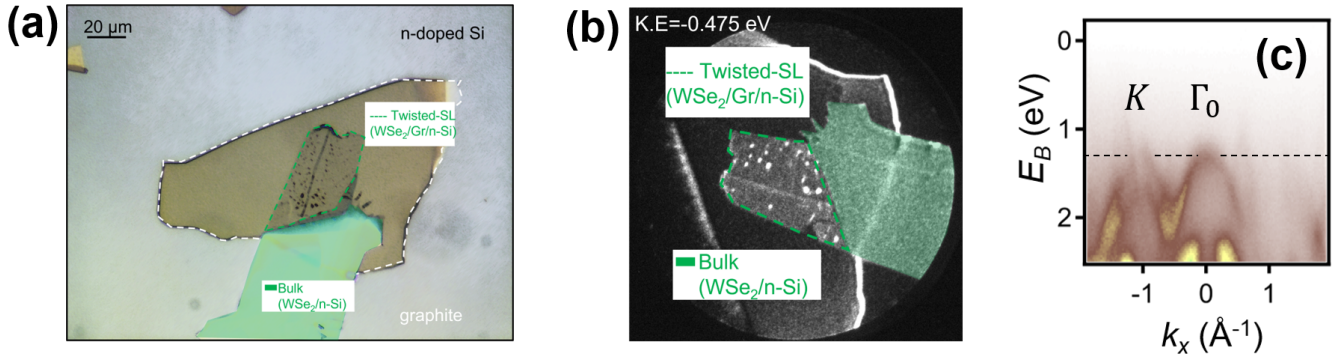

Figure S3. Overview of sample C. (a) Optical micrograph of twisted SL WSe_2 placed on graphite with the entire sample structure lying on the top of n-Si. (b) PEEM image of the sample taken with a Hg lamp at NanoESCA beamline at Elettra, where twisted SL and bulk WSe_2 flakes are represented by the dotted green lines and shaded green color regions, respectively. (c) E(k_x) map through Γ_0 indicating single band at normal emission.

SIV. ENERGY DISTRIBUTION CURVES AT Γ_0 AND K IN TWISTED BL WSE_2

To determine the band position from the ARPES data, we plotted the EDCs of the valence band dispersion at high symmetry Γ_0 and K points of twisted WSe_2 of sample B. The particular EDCs in Fig. S4(a) and (b) are related to Figs. 6 (b) and (f) of the main manuscript, respectively. At Γ_0 and K points in BL WSe_2/graphite of sample B the local VB lie respectively at $E_B \simeq 0.95$ eV and $\simeq 0.72$ eV, indicating that the global VBM in twisted WSe_2 BL resides at K point. A splitting between the topmost K bands is approx. 480 meV.

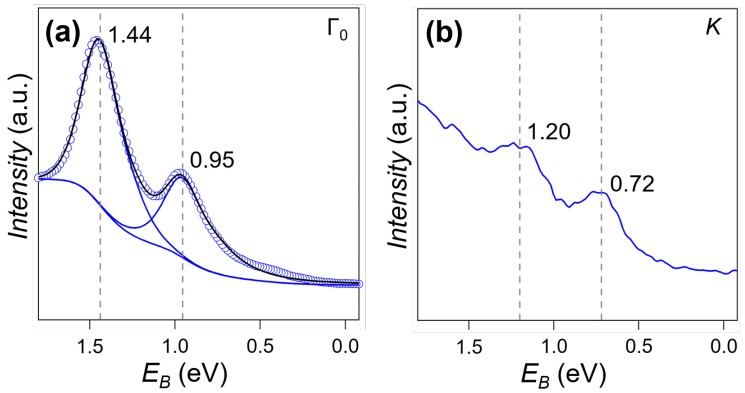

Figure S4. EDCs of twisted BL WSe_2 of sample B at Γ_0 and K.

SV. DETERMINATION OF THE TWIST ANGLE IN BL-WSE_2

ARPES studies are often limited to mapping a limited portion of the surface Brillouin zone (SBZ), and probing dispersions simultaneously in both the first and the second SBZ is not performed routinely. Since the parallel momentum $k_{||}$ depends on the emission angle θ and kinetic energy E_{kin} as $k_{||} = \sqrt{\frac{2m}{\hbar^2}E_{kin}}\sin\theta$, there are often technical limitations in reaching large enough θ at low E_{kin}, or a sufficient resolution at larger hν. The size of the SBZ depends on the lattice constant a as $2\pi/a$; therefore, for many materials, one needs to reach $k_{||} \simeq 2$ Å^{-1} to map the second SBZ, and this is, for example, out of reach using a helium discharge lamp with the He I line at $h\nu \simeq 21.2$ eV. Also momentum microscopes exhibit a limit of the maximum parallel momentum at higher E_{kin} [1], which depends on the high voltage applied between the sample and the spectrometer, which often must be limited to control the field emission. The flexibility of MAESTRO beamline allows one to use $h\nu = 147$ eV for 3D I(E_{bin}, k_x, k_y) mapping, allowing us to reach the second SBZ of WSe_2 at moderate emission angles of $\theta \simeq 20°$.

Figure S5 shows constant energy surfaces of twisted BL WSe_2/graphite of sample A and B across first and second SBZs at $E_B \simeq 0.9$ eV, where we were able to visualize the intensity pockets at Γ_0 and Γ_1 contributing from both WSe_2 monolayers that constitute the BL WSe_2 structures. The characteristic features are labeled by the white (Γ_0), red (top flake, Γ_{1top}), and green (bottom flake, $\Gamma_{1bottom}$) dotted color circles, as illustrated in Fig. S5.

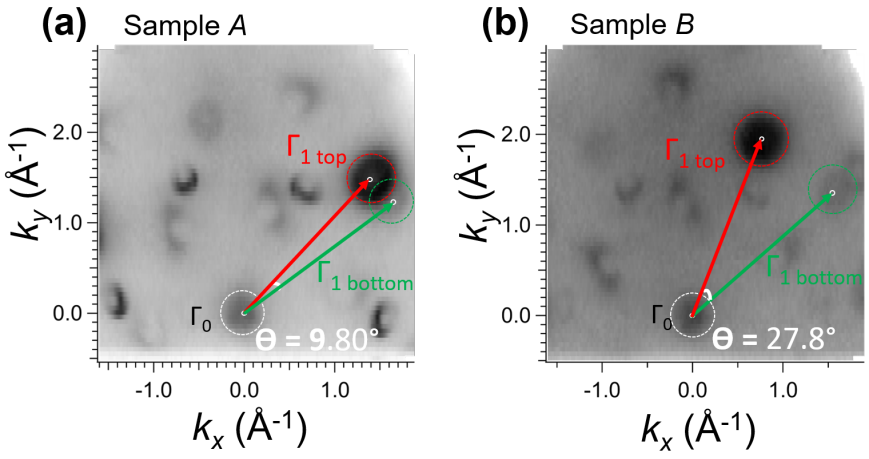

Figure S5. Panels (a) and (b) present the (k_x, k_y)-dependent constant energy maps taken at $E_B \simeq 0.9$ eV of samples A and B, respectively. The red and green arrows connect Γ_0 and Γ_{1top}, Γ_0 and $\Gamma_{1bottom}$ high symmetry points of WSe_2 bilayer structures indicating the twist angle between BL WSe_2.

Through identification of characteristic features from the top and bottom monolayers, we were able to determine the twist angles between the BL WSe_2 of sample A and B. For doing so, we utilize the band contours around the high symmetry Γ points on CEMs as illustrated in Figs. S5, S6, and S7. We mapped out the 3D I(E_B, k_x, k_y)

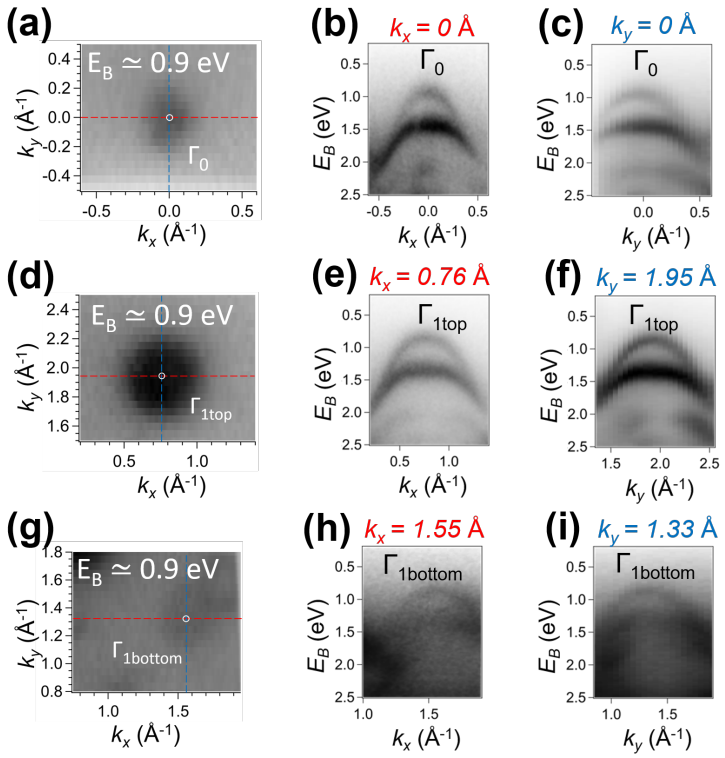

Figure S6. Sample B: (a,d,g) Constant energy contours at $E_B \simeq 0.9$ eV taken around Γ_0, Γ_{1top} and $\Gamma_{1bottom}$ respectively. (b,c,e,f,h,i) Extracted E(k_x), E(k_y) dispersions at different k_x and k_y cuts performed on all gammas, as indicated by dashed red and blue lines in (a,d,g). A white circle marking in the (a,d,g) indicates the Γ_0, Γ_{1top}, and $\Gamma_{1bottom}$ positions retrieved from the 3D dataset.

dispersion of each bilayer structures and their respective monolayers. The vectors connecting Γ_0 with Γ_{1top} and with $\Gamma_{1bottom}$ are determined by identifying the centers of Γ pockets, as illustrated in Figs. S6, and S7. The selection of the k coordinates of the high symmetry Γ points is based on a comprehensive examination of the complete (E_B, k_x, k_y)-dependent intensity of BL WSe_2 structures. We analyzed E(k_x) and E(k_y) dispersions across all the Γ pockets originating from top and bottom monolayers features in BL WSe_2 datasets of sample A and B as shown in Figs. S6 and S7. We used all the Γ pockets visualized on the CEM from the WSe_2 bilayers datasets. The intensity of the $\Gamma_{1bottom}$ is relatively low in sample A, making it difficult to select the k coordinates. For this, we approximated the coordinates from the monolayer dataset. The angle between the red and green vectors corresponds to the twist angles, which we determine as 9.80° ± 1° and 27.80° ± 1° of sample A and B as shown in Fig. S5. We note that due to non-linearities in the angular scale of the hemispherical analyzer these values very likely differ from the real twist angles, as discussed in the main text.

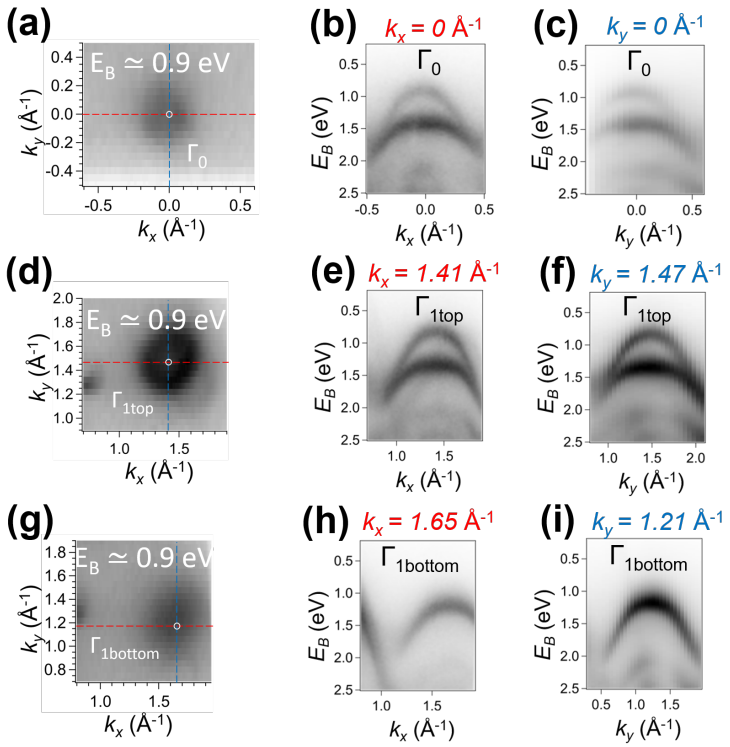

Figure S7. Same as Fig. S6 but for sample *A*.

[1] C. Tusche, A. Krasyuk, and J. Kirschner, Spin resolved bandstructure imaging with a high resolution momentum microscope, Ultramicroscopy **159**, 520 (2015).